PHYSICAL REVIEW B VOLUME 50, NUMBER 7 15 AUGUST 1994-I

Transport and level anticrossing in strongly coupled double quantum wells with in-plane magnetic fields

S. K. Lyo
Sandia National Laboratories, Albuquerque, New Mexico 87185
(Received 11 April 1994; revised manuscript received 10 June 1994)

Interesting in-plane low-temperature transport properties are proposed in doped thin double quantum wells in an in-plane magnetic field (**B**). The density of states diverges at a saddle point (SP). The SP is formed at the lower edge of the partial energy gap at a sufficiently high B due to an anticrossing of the two displaced energy-dispersion parabolas. At high carrier densities, the conductance (G) shows a maximum when the upper branch is emptied and a minimum at a higher $B=B_{\min}$ when the Fermi level lies at the SP. These features are confirmed by recent data. At low densities (i.e., with only the lower branch populated), only a G minimum is predicted to occur. The electron-diffusion thermopower diverges both above and below $B_{\min}$ with opposite signs. The correlation between the recently observed tunneling G and the in-plane G is discussed.

Currently much attention is focused on the electronic, optical, and transport properties of coupled semiconductor double-quantum-well structures (DQWS's). These DQWS's offer interesting physical properties and device concepts. Although a number of authors have studied the effect of a magnetic field (**B**) perpendicular to the quantum wells (QW's) previously, the effect of in-plane B's has received little attention. The purpose of this paper is to demonstrate theoretically some interesting electronic and low-temperature (T) transport properties induced by in-plane B's due to inter-QW tunneling.

The basic effect of an in-plane **B** ($\|\mathbf{x}$) is to displace the origins of the transverse crystal momenta k_y in the two QW's away from each other by $\Delta k_y=d/l^2$ where d is the center-to-center distance between the QW's and $l=(\hbar c/eB)^{1/2}$. In the effective-mass approximation, the energy-dispersion (ED) parabolas of the uncoupled QW's [shown by dotted curves in Fig. 1(a)] then anticross in the energy-vs-k_y plane due to tunneling, thereby introducing a gap in the k_y direc tion as shown by solid curves in Fig. 1(a). The saddle point (SP), formed at a sufficiently high B at the lower edge of the gap, yields a logarithmic singularity in the density of states (DOS). Several transport properties including the conductivity, photoluminescence line shape, and the electron-diffusion thermoelectric power (EDTEP) are sensitive to this DOS singularity. In this paper we show that, at high densities, the in-plane conductance (G) has a maximum at B when the upper branch is emptied and a minimum at a higher $B=B_{\min}$ when the Fermi level lies at the SP. On the other hand, only a single G minimum is predicted to occur at low densities with only the lower branch populated. The EDTEP diverges both above and below $B_{\min}$ with opposite signs. The B dependence of G is anisotropic with respect to the angles between **B** and the electric field (**E**). A different kind of anticrossing occurs between the two valleys in the [100] direction in a Si inversion layer. In this case, the dispersion curves are displaced in the absence of B's on vicinal surface such as (911) and interact through overlap in the **k** space.[1]

Apart from the kinetic energy in the direction of **B**, $\epsilon_x(k_x)\equiv(\hbar k_x)^2/2m^*$, the Hamiltonian is given by

$$H=\frac{p_z^2}{2m^*}+\frac{\hbar^2}{2m^*}(k_y-z/l^2)+V(z), \tag{1}$$

where the same isotropic effective mass m^* is used in the QW's and the barriers for simplicity. The confinement potential $V(z)$ in (1) is the superposition of the square-well potentials $V_1(z)$ and $V_2(z)$ of QW1 and QW2. The QW's have well widths w_1, w_2 and depths V_1, V_2, respectively. The potential energy is defined to be zero at the top of the barriers.

While the Hamiltonian in (1) can, in general, be diagonalized numerically, we consider here only approximate solutions for the lowest two sublevels in narrow QW's. Using the

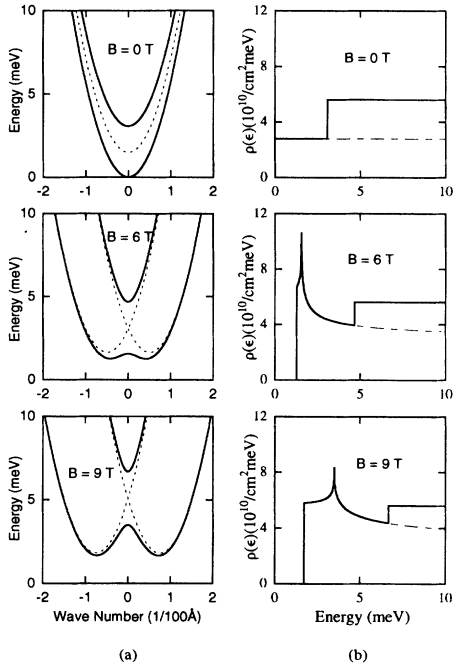

FIG. 1. (a) ED curves of a symmetric DQWS with (solid curves) and without (dashed curves) mixing. (b) The DOS from the lower (dashed curves) and both branches (solid curves).

0163-1829/94/50(7)/4965(4)/$06.00

field-free ground-sublevel eigenfunctions of the isolated single QW's $\phi_1(z)$ and $\phi_2(z)$ as the basis functions with eigenvalues ϵ_1 and ϵ_2, we find

$$\epsilon_{\pm}(k_y)=\frac{1}{2(1-S^2)}(H_{11}+H_{22}-2SH_{12}\pm\sqrt{D}) \quad (2a)$$

and

$$D=(H_{11}-H_{22})^2(1-S^2)+[(H_{11}+H_{22})S-2H_{12}]^2, \quad (2b)$$

where $S=\langle\phi_1|\phi_2\rangle$. The matrix elements are given by

$$H_{nm}=\epsilon_m\langle\phi_n|\phi_m\rangle+\langle\phi_n|V_{m'}(z)|\phi_m\rangle + \langle\phi_n|V_B(z)|\phi_m\rangle \quad (n,m=1,2), \quad (2c)$$

where the prime on the subscript m signifies that $1'=2$, $2'=1$, and $V_B(z)$ is the second term in (1).

The two energy branches $\epsilon_{\pm}(k_y)$ given in (2) are plotted in solid curves in Fig. 1(a) for several B's for a symmetric DQWS GaAs/$Al_{0.3}Ga_{0.7}As$ with $d=110$ Å, $w_1=w_2=60$ Å, $m^*=0.067m_0$ (m_0 is the free-electron mass), and $V_1=V_2=280$ meV. The dashed parabolas are the ED curves for uncoupled QW's, namely, QW1 (left side) and QW2 (right side). The two parabolas coincide at $B=0$. As a result of mixing, the parabolas repel and separate into the upper and lower branches shown in solid curves. At low B's, the bottoms of the parabolas rise very slowly as $\propto B^2\langle(z-\langle z\rangle)^2\rangle$. Here the angular brackets denote the expectation value. The SP begins to appear at a high B [i.e., above 4 T in Fig. 1(a)] because of a strong repulsion between the two branches.

The ED near the SP of the lower branch is of the form $\epsilon(k_x,k_y)=\epsilon_0+(\hbar k_x)^2/2m^*-(\hbar k_y)^2/2m'$ where m' (>0) is determined from the curvature at the SP and ϵ_0 is the energy at the SP. This type of ED [i.e., with a negative sign for the last term of $\epsilon(k_x,k_y)$] yields a Van Hove singularity for the DOS of the form $\rho(\epsilon)\propto-\ln|\epsilon-\epsilon_0|$. The DOS is shown in Fig. 1(b) for several B's. The singularity is clearly seen there and moves up with B in accordance with the behavior of the SP shown in Fig. 1(a). The separation between the singularity peak and the DOS step (of the upper branch) in Fig. 1(b) is mainly determined by mixing and is insensitive to B.

For an asymmetric DQWS, there are two different types of crossing (i.e., types I and II) of the parabolas depending on the magnitude of B. In type-I crossing, B is low so that the bottom of the upper parabola is inside the lower parabola and therefore the slopes of the tangents to the parabolas at the crossing point have the same sign. In contrast, in type-II crossing, B is high so that the bottom of the upper parabola is outside the lower parabola and therefore the slopes have opposite signs. These properties are demonstrated in the bottom row of Fig. 2 at two different B's, namely, at 2 T [Fig. 2(b)] and 6 T [Fig. 2(c)] for a DQWS with $d=140$ Å, $w_1=w_2=60$ Å, $V_1=280$ meV, and $V_2=277$ meV. Although only the anticrossing of the parabolas is shown in these figures for the sake of clarity, type-I and type-II crossings of the noninteracting parabolas can easily be seen in the bottom row of Figs. 2(b) and 2(c). It is seen in the top row that the DOS singularity appears only in the 6-T figure but not in the 2-T figure. In this weakly coupled DQWS, the zero-B splitting

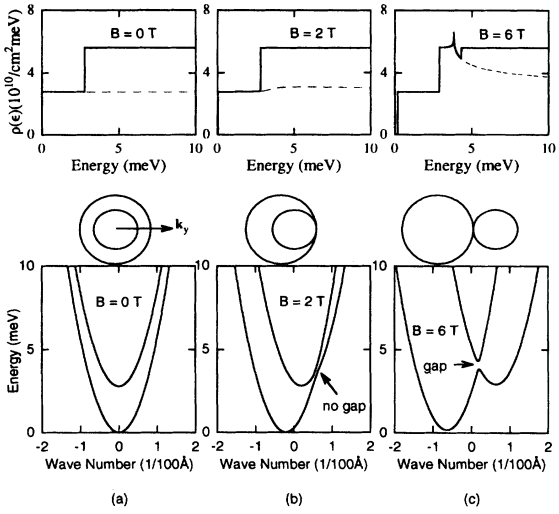

FIG. 2. ED curves of an asymmetric DQWS at (a) $B=0$ T, (b) $B_-=2$ T, and (c) $B_+=6$ T (bottom row). The circles on the middle row are the Fermi circles of QW1 and QW2. The top row shows the DOS from the lower (dashed curves) and both branches (solid curves).

between the upper and lower branches in Fig. 2(a) is mainly due to different well depths unlike in Fig. 1. In Figs. 2(a) and 2(b), the crossing occurs at the Fermi level.

The concomitant Fermi surfaces (FS's) of the same asymmetric DQWS are schemtically shown in the middle row, ignoring mixing (i.e., for weakly coupled QW's with a wide barrier between them). In type-I crossing, the two FS's touch from inside at the lower field $B\equiv B_-$ as in Fig. 2(b) and the anticrossing only distorts the ED curves without opening a gap. On the other hand, the FS's touch from outside at the higher field $B\equiv B_+$ in type-II crossing as illustrated in Fig. 2(c) and a gap is opened in the transverse direction. At a sufficiently high B, a SP and therefore a Van Hove singularity of the DOS appear on the FS. Sharp resonance peaks were observed recently at $B=B_-$ and B_+ for the *tunneling* G between QW1 and QW2.[2,3] These peaks arise from the fact that a maximum number of states in QW1 and QW2 satisfy both the momentum- and energy-conservation conditions for resonance tunneling when the two Fermi circles touch each other tangentially as shown in the middle row of Figs. 2(b) and 2(c).

The singularity in the DOS at the FS introduces divergence in the in-plane resistance. The in-plane G in the direction $\mathbf{u}=\mathbf{E}/|\mathbf{E}|$ is given, in the relaxation-time ($\tau_{\mathbf{k}}$) approximation, by $G=(2e^2/A)\sum(\mathbf{u}\cdot\mathbf{v}_{\mathbf{k}})^2[-f'_{\mathbf{k}}]\tau_{\mathbf{k}}$ where $\mathbf{v}_{\mathbf{k}}=\hbar^{-1}\nabla_{\mathbf{k}}\epsilon_{\mathbf{k}}$, $\epsilon_{\mathbf{k}}=\epsilon_x(k_x)+\epsilon_{\pm}(k_y)$ and A is the area of the cross section of the QW's. The prime on the Fermi function $f_{\mathbf{k}}\equiv f(\epsilon_{\mathbf{k}})$ denotes the first derivative with respect to the energy. For delta-potential impurities (e.g., surface roughness or short-range impurity potentials) and a symmetric DQWS, $\tau_{\mathbf{k}}$ is approximated by

$$\tau_{\mathbf{k}}^{-1}=\frac{2\pi N_I}{\hbar}\sum_{\mathbf{k}'}\langle|V_{\mathbf{k}',\mathbf{k}}(z_i)|^2\rangle\delta(\epsilon_{\mathbf{k}}-\epsilon_{\mathbf{k}'}). \quad (3)$$

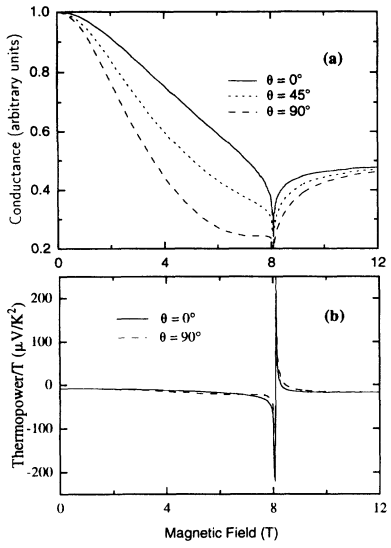

FIG. 3. (a) The conductance and (b) the EDTEP/T vs B for the DQWS studied in Fig. 1. θ is the angle between the electric field (∇T) and $\mathbf{B}$ for the conductance (EDTEP).

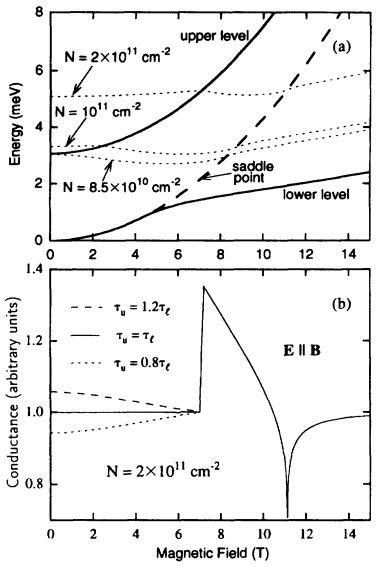

FIG. 4. (a) The bottoms of the two branches (solid curves) and the SP (long-dashed curve) vs B for the DQWS studied in Fig. 1. The Fermi levels are shown in short-dashed curves. (b) G vs B.

Here $V_{\mathbf{k}',\mathbf{k}}(z_i)$ represents the matrix element of the potential from an impurity at $z=z_i$ and has a slow momentum dependence through B-induced k_y-sublevel mixing. The $\mathbf{k}$ and $\mathbf{k}'$ summations include both branches. While the so-called scattering-in-term correction is necessary in (3) in general, this correction is not expected to change the qualitative results of the present paper. The scattering-in term in (3) cancels out in the special case where the impurities are at the center of the middle barrier because $\langle|V_{-\mathbf{k}',\mathbf{k}}(z_i)|^2\rangle = \langle|V_{\mathbf{k}',\mathbf{k}}(z_i)|^2\rangle = \langle|V_{\mathbf{k}',-\mathbf{k}}(z_i)|^2\rangle$. Here, the angular brackets denote averaging over the impurity distribution. In (3), N_I is the total number of the static scattering centers randomly distributed in the x-y directions but according to a certain probability distribution in the growth direction. Approximating $V_I^2 \equiv \langle V_{\mathbf{k}',\mathbf{k}}(z_i)^2\rangle$, we find $\tau(\epsilon_{\mathbf{k}})^{-1} \approx \pi\, V_I^2 N_I \rho(\epsilon_{\mathbf{k}})/\hbar$ where $\rho(\epsilon_{\mathbf{k}})$ is the DOS (ignoring the spin splitting). The EDTEP is given by Mott's formula $Q = (\pi^2 k_B^2 T/3d)d\ \ln G(\epsilon_F)/d\epsilon_F$, where ϵ_F is the Fermi energy and e is negative for electrons.

The zero-temperature G and EDTEP obtained from this approximation are shown in Fig. 3 for the symmetric DQWS studied in Fig. 1 with $N=8.5\times10^{10}$ cm^{-2} as a function of B. At this density, the Fermi level is just below the bottom of the upper branch at $B=0$ [see Fig. 4(a)]. The SP sweeps across the Fermi level as B is increased. The vanishing in-plane G at $B_+\approx8.1$ T in Fig. 3(a) arises from the fact that the SP lies on the FS, which has a figure-8 shape with the SP at the center and with its vertical symmetry axis in the k_y direction. In this case, the electrons on the FS are scattered into the SP region with a divergent rate because of the divergent DOS from this area, yielding $G=0$. Note that the electrons in these states at the SP do not contribute to additional current because they move with zero velocities (i.e., $\mathbf{v}_{\mathbf{k}}=0$). The damping of the levels is expected to round out the sharp minimum in Fig. 3(a). In contrast to the in-plane G, the tunneling G is expected to reach a second maximum around $B_+\approx8.1$ T according to the argument presented earlier. For an asymmetric DQWS, the in-plane G does not vanish at type-I crossing, where the first peak of the tunneling G appears. Recent preliminary data of Simmons *et al.*[4] indicate this kind of correlation between the in-plane and tunneling G. In Fig. 3(a), the longitudinal G is larger than the transverse G because the projection of the FS weighted by the x component of the Bloch velocity is larger in the direction of $\mathbf{B}$ than in the transverse direction.

The EDTEP in Fig. 3(b) diverges above and below $B\simeq8.1$ T with opposite signs according to $Q=(\pi^2k_B^2T/3e)[(\epsilon_0-\epsilon_F)\ln|\epsilon_0-\epsilon_F|]^{-1}$. The divergence occurs because the EDTEP is proportional to the derivative of the scattering rate and therefore the DOS with respect to the Fermi energy according to Mott's formula. Below $B\simeq8.1$ T, the Fermi energy lies above the SP and the DOS has a negative slope as seen in Fig. 1, yielding a *negative* EDTEP for electrons. On the other hand, the Fermi level lies below the SP for fields >8.1 T and the DOS has a positive slope, yielding a *positive* EDTEP. The phonon-drag contribution to the TEP is usually important only at temperatures greater than 1 K.[5]

At high carrier densities (i.e., with both branches populated at $B=0$), G shows not only the SP-induced sharp minimum (e.g., around 11.1 T) but also a strong maximum at a lower B (around 7.2 T) as displayed in Fig. 4(b) for the same symmetric DQWS studied in Fig. 3 with a higher density $N=2\times10^{11}$ cm^{-2}. In Fig. 4(a), the Fermi levels are shown for several densities. The (short-dashed) curves show gentle cusps when they intersect the solid curve representing the bottom of the upper branch because of the sharp steplike drop of the DOS along this curve. The G maximum at 7.2 T in Fig. 4(b) follows from the sudden depopulation of carriers from the bottom of the upper branch [see Fig. 1(b)] at this B; although these slow-velocity states (i.e., $\mathbf{v}_{\mathbf{k}}\simeq\mathbf{0}$) carry little current, they provide a large number of states for the FS

carriers to be scattered into elastically, reducing the scattering times. Therefore, carrier scattering times increase suddenly above the depopulation field, yielding a sharp increase in G. In Fig. 4(b), the three curves are obtained for different ratios of the scattering rates of the upper (τ_u^{-1}) and lower (τ_l^{-1}) branches, which are assumed to be proportional to the total DOS. A more realistic expression for τ_u^{-1} and τ_l^{-1} depends on the nature and the distribution of the scattering centers. For example, G calculated from (3) for two sheets of delta-function impurities located at any of the two GaAs-$Al_xGa_{1-x}As$ or $Al_xGa_{1-x}As$-GaAs interfaces is similar to the $\tau_u = \tau_l$ curve.

In summary, we have examined the effect of a Van Hove singularity arising from a level anticrossing in an external in-plane B. We found that G shows a maximum and a minimum as a function of B at high densities (with both branches populated) and a single minimum at low densities (with only the lower branch populated). The maximum-minimum feature is consistent with the behavior recently observed by Simmons *et al.* in $GaAs/Al_{0.3}Ga_{0.7}As$ DQWS's.[4] The shape of the FS changes continually with increasing B and can be studied using the de Haas–Shubnikov effect.[6] The correlation between the recently observed[4] tunneling G and the in-plane G was discussed. The thermopower diverges both above and below B_{min} with opposite signs.

Note added in proof. The maximum and minimum of the B-dependent G correspond to the maximum and minimum of the density-dependent G found earlier by Ando in a vicinal Si inversion layer.[7]

The author thanks Dr. J. A. Simmons for valuable discussions on the subject. This work was supported by U.S. DOE under Contract No. DE-AC04-94AL85000.

[1] For a review and references, see T. Ando, A. B. Fowler, and F. Stern, Rev. Mod. Phys. **54**, 437 (1982).

[2] J. P. Eisenstein, T. J. Gramila, L. N. Pfeiffer, and K. W. West, Phys. Rev. B **44**, 6511 (1991).

[3] J. A. Simmons, S. K. Lyo, J. F. Klem, M. E. Sherwin, and J. R. Wendt, Phys. Rev. B **47**, 15 741 (1993).

[4] J. A. Simmons, S. K. Lyo, N. E. Harff, and J. F. Klem (unpublished).

[5] R. Fletcher, J. C. Maan, and G. Weiman, Phys. Rev. B **32**, 8477 (1985); S. K. Lyo, Phys. Rev. B **38**, 6345 (1988).

[6] G. S. Boebinger, A. Passner, L. N. Pfeiffer, and K. W. West, Phys. Rev. B **43**, 12 673 (1991).

[7] T. Ando, J. Phys. Soc. Jpn. **47**, 1595 (1979).